

G-13

4895/2-77



ОБЪЕДИНЕННЫЙ
ИНСТИТУТ
ЯДЕРНЫХ
ИССЛЕДОВАНИЙ

ДУБНА

12/xII-77

E7 - 10880

H.Gaeggeler, A.S.Iljinov, G.S.Popeko, W.Seidel,
G.M.Ter-Akopian, S.P.Tretyakova

A STUDY OF FUSION REACTIONS
BETWEEN $^{206,207}\text{Pb}$ NUCLEI
AND ^{40}Ar IONS
NEAR THE COULOMB BARRIER

1977

E7 - 10880

**H.Gaeggeler, A.S.Iljinov,* G.S.Popeko, W.Seidel,
G.M.Ter-Akopian, S.P.Tretyakova**

**A STUDY OF FUSION REACTIONS
BETWEEN $^{206,207}\text{Pb}$ NUCLEI
AND ^{40}Ar IONS
NEAR THE COULOMB BARRIER**

Submitted to "Nuclear Physics"

* Institute of Nuclear Research, Moscow, USSR

Геггелер Х. и др.

E7 - 10880

Исследования реакций слияния $^{206,207}\text{Pb}$ с ионами ^{40}Ar вблизи кулоновского барьера

Измерены функции возбуждения реакций $^{206}\text{Pb}(^{40}\text{Ar},2n)^{244}\text{Fm}$ и $^{207}\text{Pb}(^{40}\text{Ar},3n)^{244}\text{Fm}$. Результаты проанализированы в рамках статистической модели. Получены параметры оптического потенциала ($V_0 = -70$ МэВ, $r_0 = 1,26 \cdot 10^{-13}$ см, $d = 0,36 \cdot 10^{-13}$ см). С этим набором параметров рассчитана зависимость сечения слияния от энергии иона и определен барьер слияния. Из абсолютных сечений α -реакций получена усредненная по испарительному каскаду делимость составных ядер.

Работа выполнена в Лаборатории ядерных реакций ОИЯИ.

Препринт Объединенного института ядерных исследований. Дубна 1977

Gaeggeler H. et al.

E7 - 10880

A Study of Fusion Reactions Between $^{206,207}\text{Pb}$ Nuclei and ^{40}Ar Ions Near the Coulomb Barrier

Excitation functions for the reactions $^{206}\text{Pb}(^{40}\text{Ar},2n)^{244}\text{Fm}$ and $^{207}\text{Pb}(^{40}\text{Ar},3n)^{244}\text{Fm}$ have been measured and analysed in terms of a statistical model. The optical potential parameters have been found as follows: $V_0 = -70$ MeV, $r_0 = 1.26 \times 10^{-13}$ cm, and $d = 0.36 \times 10^{-13}$ cm. Some data on the properties of the excited compound nucleus of fermium have been obtained.

The investigation has been performed at the Laboratory of Nuclear Reactions, JINR.

Preprint of the Joint Institute for Nuclear Research. Dubna 1977

1. INTRODUCTION

Studies of heavy-ion induced reactions leading to highly fissionable isotopes of transfermium elements are very important for investigating the mechanism of nuclear reactions and resolving the problem of synthesis of superheavy elements. To produce isotopes of this region one has used and investigated reactions involved in the bombardment of uranium, plutonium and still heavier targets up to berkelium with ion ranging from boron to neon.

Recently a new method of element production has been developed which employs complete fusion reactions between heavy ions $A \geq 40$ with lead, thallium or bismuth isotopes^{/1/} to produce nuclei with $Z \geq 100$. An advantage of this technique is that the compound nuclei produced have a minimum excitation energy compared with other target-projectile combinations. A number of reactions with heavy ions from ^{40}Ar to ^{58}Fe have been investigated previously^{/1-6/}, and the cross sections corresponding to the excitation function maxima have been obtained. An analysis of the shapes of excitation functions for these reactions may provide more detailed information on their mechanism.

In the present paper the excitation functions of the two reactions $^{206}\text{Pb}(^{40}\text{Ar},2n)^{244}\text{Fm}$ and $^{207}\text{Pb}(^{40}\text{Ar},3n)^{244}\text{Fm}$ have been investigated.

2. DESCRIPTION OF EXPERIMENTS

The experiments were carried out using an argon external ion beam from the U-300 heavy ion cyclotron. The final product of the reactions studied, ^{244}Fm , undergoes spontaneous fission with a 100% probability and has a half-life of about 4 ms^{1,7/}. These properties of ^{244}Fm permitted its detection using a comparatively simple technique as follows. Recoil nuclei knocked out from the target were stopped in a rotating disk and transported to mica detectors of spontaneous fission fragments. The rotating disk was made of aluminium foil 9 μm thick. The diameter of the disk was equal to 185 mm, and the rotation rate was 8300 rev/min. The mica detectors were placed on both sides of the collecting disk parallel with its surface. The detection efficiency for spontaneous fission fragments was about 50%.

The targets prepared from separated lead isotopes (the isotopic composition of the targets is given in table 1) had the form of thin 0.4-1.2 mg/cm² metallic layers deposited onto nickel backing foils 0.8-1.4 mg/cm² thick. These lead layers with the backing foil were mounted on a disk rotating with a velocity of 200 rev/min. To increase radiation the target was covered with 20 $\mu\text{g}/\text{cm}^2$ carbon layers on both sides. Such a design of the target permitted the use of

Table 1
Isotopic composition of targets

Target	Isotopic contents, %			
	^{204}Pb	^{206}Pb	^{207}Pb	^{208}Pb
^{206}Pb	-	90.4	6.7	2.9
^{207}Pb	0.2	1.7	87.9	10.2

intensive argon ion beams. No target substance losses were observed at the argon ion flux of up to 1.5×10^{12} per/sec and integral flux of up to 10^{18} ions.

The thickness of the lead layers was measured before and after the bombardments by weighting and measuring the ^{241}Am α -particle energy absorbed by the target. In addition, the lead quantity was controlled by the X-ray fluorescence analysis. The measurement error did not exceed 5%.

The initial argon ion energy of (221±2) MeV was varied by aluminium and nickel degraders. The degraders were also fixed on the rotating disk. The energy of the ^{40}Ar ions incident on the target was calculated using tables of ref. /8/

The beam intensity was checked using a Faraday cup. In addition, the integral flux of argon nuclei was measured from the yield of products of the complete fusion reaction $\text{Cd} + ^{40}\text{Ar}$. For this purpose cadmium foil strips were fixed on the disk with degrading foils and on the recoil catheter foil. The particle flux incident on these strips was approximately 1% of the total flux arriving at the

target. The error in the determination of the absolute value of the integral flux was up to 10%.

3. EXPERIMENTAL RESULTS

The results of the experiments performed are presented in table 2. The thickness of the degrading foils used to vary the beam energy is given in the first row of the table. Data on the beam energy on the target are given in the second row. The energy ranges given include the beam energy spread following passage through degraders and energy losses in the target. The numbers of spontaneous fission events detected in each experiment are given in the fifth row. The next row gives the corrected number of spontaneous fission events due to ^{244}Fm . The introduction of corrections is conditioned by the fact that contributions to the observed spontaneous fission come not only from the main reaction $^{206}\text{Pb}(^{40}\text{Ar},2n)^{244}\text{Fm}$ or $^{207}\text{Pb}(^{40}\text{Ar},3n)^{244}\text{Fm}$, but also from other reactions occurring on the admixture lead isotopes contained in the targets (see table 1) and on the main isotope, leading to the formation of another spontaneously fissioning isotope of fermium. In the case of the main reaction $^{206}\text{Pb}(^{40}\text{Ar},2n)^{244}\text{Fm}$, the following background reactions were taken into account: $^{207}\text{Pb}(^{40}\text{Ar},3n)^{244}\text{Fm}$, $^{206}\text{Pb}(^{40}\text{Ar},4n)^{242}\text{Fm}$ and $^{208}\text{Pb}(^{40}\text{Ar},4n)^{244}\text{Fm}$, whereas for the reaction $^{207}\text{Pb}(^{40}\text{Ar},3n)^{244}\text{Fm}$ the reactions $^{206}\text{Pb}(^{40}\text{Ar},2n)^{244}\text{Fm}$, $^{206}\text{Pb}(^{40}\text{Ar},4n)^{242}\text{Fm}$ and $^{208}\text{Pb}(^{40}\text{Ar},4n)^{244}\text{Fm}$ were taken into account. In making corrections we used the data presented in refs.^{1,3/}. The background due to fission of ^{246}Fm produced

Table 2. Experimental results

Thickness of degrading foils, mg/cm ²	Bombarding energy, MeV	Integral ion flux x10 ¹⁶	Target thickness, mg/cm ²	Number of detected fission events	Corrected number of s.f. events	σ (cm ²)
$^{206}\text{Pb}(^{40}\text{Ar}, 2n)^{244}\text{Pm}$						
2.2 Al+1.4 Ni	178 \pm 5	2.8	1.2	—	—	< 1.3x10 ⁻³⁵
2.2 Al+1.0 Ni	183 \pm 3	2.1	0.7	I	I	(6 \pm 6)x10 ⁻³⁵
1.6 Al+1.4 Ni	185 \pm 4	5.6	1.2	96	96	(1.2 \pm 0.2)x10 ⁻³³
1.3 Al+1.3 Ni	190 \pm 3	5.8	0.5	64	64	(1.7 \pm 0.2)x10 ⁻³³
2.2 Al	193 \pm 3	1.4	0.4	18	17	(2.8 \pm 1.4)x10 ⁻³³
2.3 Ni	196 \pm 3	3.0	0.7	16	11	(4.4 \pm 1.3)x10 ⁻³⁴
1.4 Ni	204 \pm 3	6.7	1.2	23	7	(7 \pm 3)x10 ⁻³⁵
$^{207}\text{Pb}(^{40}\text{Ar}, 3n)^{244}\text{Pm}$						
1.6 Al+0.8 Ni	191 \pm 3	2.5	0.7	44	39	(1.9 \pm 0.4)x10 ⁻³³
2.2 Ni	197 \pm 3	2.2	0.7	70	64	(4.2 \pm 0.7)x10 ⁻³³
1.8 Ni	201 \pm 3	4.5	0.7	118	109	(3.5 \pm 0.4)x10 ⁻³³
0.8 Ni	211 \pm 2	3.3	0.7	53	49	(1.8 \pm 0.4)x10 ⁻³³
	219 \pm 2	5.4	0.7	6	6	1.2 \pm 0.6)x10 ⁻³⁴

in the reaction $^{208}\text{Pb}(^{40}\text{Ar}, 2n)$ was neglected since it was equal to 1 to 3% of the total number of fission fragments.

In the experiments performed we have detected a total of 510 spontaneous fission events due to ^{244}Fm . The time distribution of these events corresponded to the decay of an activity with a half-life of (3.0 ± 0.5) ms (see fig. 1). This is in good agreement with the data on ^{244}Fm (refs. ^{1,77}).

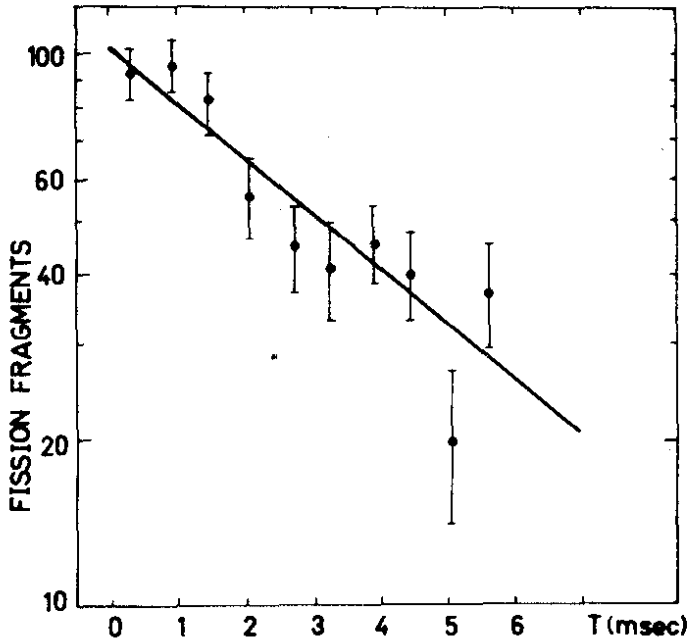


Fig. 1. Time distribution of spontaneous fission fragments due from ^{244}Fm .

The cross sections calculated on the basis of the experimental data are presented in the last row of table 2. In fig. 2 these cross sections are shown as excitation functions. The errors indicated for the cross sections in table 2 and fig. 2 include only

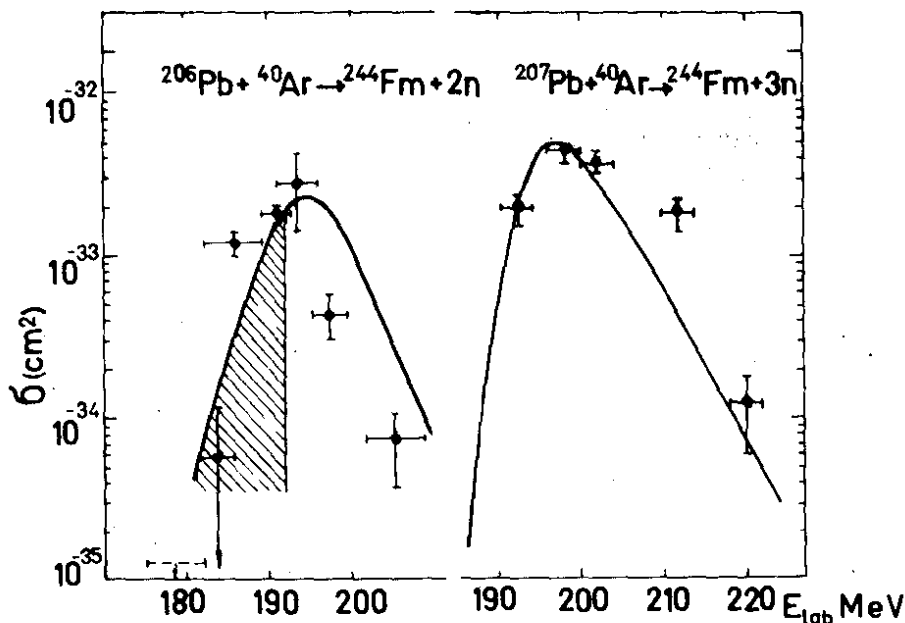


Fig. 2. Excitation functions of the reactions $^{206}\text{Pb}(^{40}\text{Ar},2n)^{244}\text{Fm}$, $^{207}\text{Pb}(^{40}\text{Ar},3n)^{244}\text{Fm}$. Calculated excitation curves (relative units) are shown by solid lines. The dashed area corresponds to the subbarrier energies of argon projectiles.

the counting statistics and inaccuracies in the target thickness determination. The absolute values of cross sections should be determined taking into account the systematic

errors due to the measurement of the integral ion flux and the spontaneous fission fragment detection efficiency. These errors are estimated to make up 40-50%.

4. DISCUSSION OF RESULTS

An analysis of the measured excitation functions permits derivation of information on the fusion process between two nuclei and the properties of the compound nucleus formed. Since the process involving the evaporation of a minimum number of neutrons takes place in the vicinity of the fusion threshold, the left-hand slope of the excitation function of the $2n$ reaction determined one of the main characteristics of fusion, its threshold. The width of the excitation functions and the slope of their high-energy "tails" determine the character of the neutron evaporation process. Finally the absolute values of cross sections for the evaporation of x neutrons allow one to obtain the value of the fissility parameter of the compound nucleus. Such an analysis of the data may be carried out using the known method of calculating the (HI, xn) reactions, described in detail in refs. ^{9,10}.

The dependence of the cross section of the xn reaction on the bombarding energy E is described by the relation

$$\sigma_x(E) = \left\{ \prod_{i=1}^x \frac{\Gamma_n}{\Gamma_f} \right\}_i \sigma_{CN} \cdot P_x = \left\{ \prod_{i=1}^x \left(\frac{\Gamma_n}{\Gamma_f} \right)_i \right\} \sum_{L=0}^{L_{CN}} \sigma_L P_{x,L}(E^*), \quad (1)$$

where the expression in parentheses determines the fraction of the initial number of the compound nuclei escaping fission. The quantity $P_{x,L}(E^*)$ denotes the probability of emission of x neutrons from the compound nucleus with an angular momentum L and excitation energy E^* . Summation of partial cross sections is made over all partial waves up to the critical value determined by the empirical relation

$$\frac{\sigma_{CN}}{\sigma_{inel}} = \frac{\sum_{L=0}^{L_{CN}} \sigma_L}{\sum_{L=0}^{\infty} \sigma_L} = \frac{1}{1+0,03 A_I} \quad (2)$$

According to this relation the contribution of the compound nucleus formation channels to the total inelastic reaction cross section decreases as the ion mass A_I increases; for reactions induced by ^{40}Ar ions the fusion cross section σ_{CN} makes up only 45% of σ_{inel} .

a) The fusion threshold B_{fus}

In ref. ^{/1/} it was shown that the cross sections of the 2^n and 3^n reactions are very sensitive to the minimum values of the compound nucleus excitation energy which is defined by the expression

$$E_{min}^* = B_{fus} + M_I + M_T - M_{CN} \quad (3)$$

One may take advantage of this circumstance to determine the value of the fusion threshold for nuclei with masses taken to be equal to the well known experimental values.

In our calculation the dependence of σ_x on B_{fus} is introduced by the partial cross section σ_L which is determined by the equation

$$\sigma_L = \pi \lambda^2 (2L+1) T_L, \quad (4)$$

where T_L is the transmission coefficient of the L -th wave through the potential $V_L(r)$ between the interacting nuclei

$$V_L(r) = \frac{Z_I Z_T e^2}{r} + \frac{\hbar^2 L(L+1)}{2\mu r} + V_0 \exp \frac{r_0 (A_I^{1/3} + A_T^{1/3}) - r}{d}. \quad (5)$$

The left-hand slope of the excitation function for the reaction $^{206}\text{Pb}(^{40}\text{Ar}, 2n)^{244}\text{Fm}$ is best fitted to the following values of the optical potential parameters: $V_0 = -70$ MeV, $r_0 = 1.26 \times 10^{-13}$ cm and $d = 0.36 \times 10^{-13}$ cm (see fig. 2). This set of parameters makes it possible to calculate the dependence of the fusion cross section on the ion energy (fig. 3) and hence determine the fusion barrier.

It is worthwhile comparing the above described method of determining the fusion barrier with the traditional way based on the direct measurement of the fusion cross section σ_{CN} . It should be noted that the first point on the excitation function for the reaction $^{206}\text{Pb}(^{40}\text{Ar}, 2n)$ corresponds to the energy at which the fusion cross section is a factor of 10^5 - 10^6 smaller than its maxi-

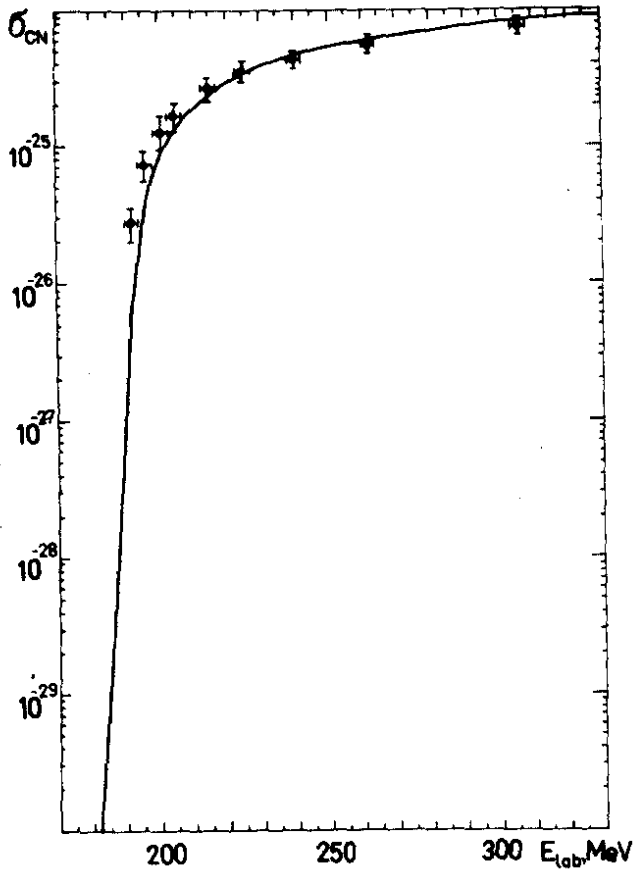


Fig. 3. Cross section of the fusion reaction $^{206}\text{Pb} + ^{40}\text{Ar}$ as function of bombarding energy. The points show experimental values (relative units) of the cross section for the fusion reaction $^{208}\text{Pb} + ^{40}\text{Ar}$, taken from ref. ^{/11/}

mum value (see fig. 3). At the same time the direct measurements of fusion cross sections ^{/11/} show a factor of 10^2 variation in σ_{CN} . This requires the extrapolation of the data

to the region of low energies, i.e., the assumption that the shape of the functional dependence of $\sigma_{CN}(E)$ is the classical one:

$$\sigma_{CN} = \pi r_{\text{eff}}^2 (A_I^{1/3} + A_T^{1/3}) \left(1 - \frac{B_{\text{fus}}^{\text{c.m.}}}{E_{\text{c.m.}}}\right). \quad (6)$$

The value of the fusion threshold is determined using the linear extrapolation of $\sigma_{CN} = f(1/E_{\text{c.m.}})^{12/}$. Further B_{fus} is parameterized as follows

$$B_{\text{fus}} = \frac{Z_I Z_T e^2}{r_{\text{eff}} (A_I^{1/3} + A_T^{1/3})}. \quad (7)$$

The calculation (fig. 4) however shows that in the region of low energies near the fusion barrier the fusion cross section should strongly differ from the classical dependence (7). This difference is due to the quantum-mechanical effect of barrier penetration, which, in turn, depends on the barrier shape.

It is interesting to note that the linear extrapolation of the quantum-mechanical dependence $\sigma_{CN} \left(\frac{1}{E_{\text{cm}}}\right)$ in fact results in the true fusion barrier height, $B_{\text{fus}} = 162.3 \text{ MeV}$ ($r_{\text{eff}} = 1.404 \text{ fm}$) (see figs. 4 and 5). From fig. 5 one can also see that half of the excitation function for the reaction $^{208}\text{Pb}(^{40}\text{Ar}, 2n)$ corresponds to the subbarrier energies of bombarding ions. The measurement of the excitation function for the subbarrier $2n$ reaction permits derivation of information not only on the height but also on the shape of the Coulomb barrier.

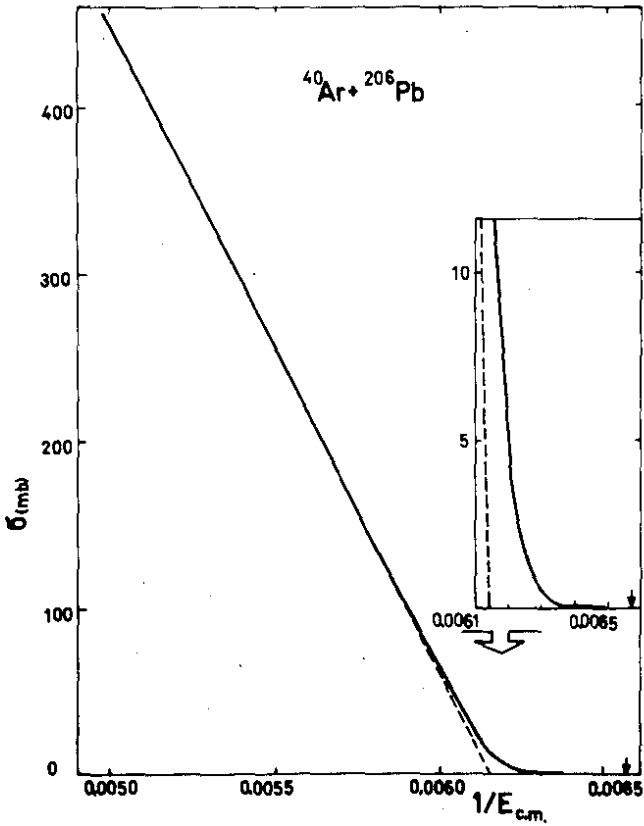


Fig. 4. Deviation of the quantum-mechanical calculation for the fusion cross section (solid line) from the classical dependence (6). The insert shows the small-energy region near the threshold on an enlarged scale.

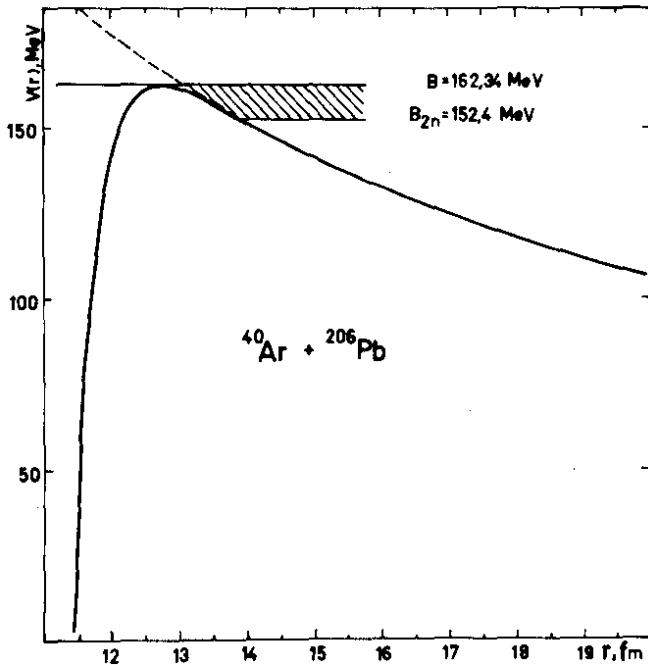


Fig.5. The potential $V_0(r)$ of nuclear interaction between ^{40}Ar and ^{206}Pb . Half of the excitation function of the reaction $^{206}\text{Pb}(^{40}\text{Ar},2n)$ corresponds to the subbarrier energies of Ar projectiles (shaded area).

b) Features of neutron evaporation from the compound nucleus

The position of the maximum of the excitation function, its width and the slope of the high-energy tail are mainly defined by the function

$$P_{x,L}(E^*) = \Gamma(\Delta_x, 2x-3) - \Gamma(\Delta_{x+1}, 2x-1). \quad (8)$$

Here $\Gamma(z,n)$ is incomplete gamma function whose arguments take on the values

$$\Delta_x = (E^* - \sum_{i=1}^x B_i - \frac{\hbar^2 L(L+1)}{2J}) / T,$$

$$\Delta_{x+1} = (E^* - \sum_{i=1}^x B_i - B_{x+1}^f - \frac{\hbar^2 L(L+1)}{2J}) / T, \quad (9)$$

which are dependent on the neutron binding energies B_i , the fission barrier B_{x+1}^f , temperature T and the moment of inertia of the nucleus J .

An analysis of numerous data on compound nucleus decay in reactions induced by C, N, O, Ne and Ar ions has shown that in these cases the particle emission has a statistical character (see, e.g., ref.^{/19/}). In the region of heavy compound nuclei, the following parameters were found: $T = 1.2$ MeV and $J = 0.8 J_{\text{rig. body}}^{\text{/9.10/}}$. The measured excitation functions for the reactions $\text{Pb}(\text{Ar}, 2n)$ and $\text{Pb}(\text{Ar}, 3n)$ are well describable by this set of parameters (see fig. 2). This indicates that the neutron emission process from the compound nucleus has an equilibrium character even in the case of such a small number of neutrons emitted, $x=2-3$.

c) The fissility parameter of the compound nucleus

From the absolute values of cross sections for the xn reactions one can find the averaged fissility parameter of compound nuclei using the relation

$$\left\langle \frac{\Gamma_n}{\Gamma_f} \right\rangle = \left(\frac{\sigma_x^{\text{exp}}}{\sigma_{\text{CN}}^{\text{P}_x}} \right)^{1/x} \quad (10)$$

The obtained values of the fissility parameter for the different isotopes of Fm , produced in reactions with ions of C, N, O, Ne and Ar are shown in fig. 6. In reactions induced by Ar ions the errors given near the experimental points reflect the influence of an uncertainty in the parameter $d = (0.36 \pm 0.01)$ fm, which was varied to fit to the excitation function shape.

In the region of neutron-deficient nuclei, the dependence of Γ_n/Γ_f on mass number A of Fm isotopes is describable by the relation

$$\log \Gamma_n / \Gamma_f = 0.14N - 22.26. \quad (11)$$

The results presented suggest that the reaction $\text{Pb} + \text{Ar}$ may lead to the formation of a compound nucleus whose decay has an equilibrium and statistical character. The conclusions drawn in the present paper will allow one to predict the cross sections for the complete fusion reactions leading to the formation of fissioning transfermium element nuclei.

In conclusion the authors take pleasure in acknowledging the constant interest in the work and useful discussions with Professors G.N.Flerov and Yu.Ts.Oganessian. Thanks are also due to K.I.Merkina and L.V.Djolos for their assistance in the treating and scanning of mica detectors.

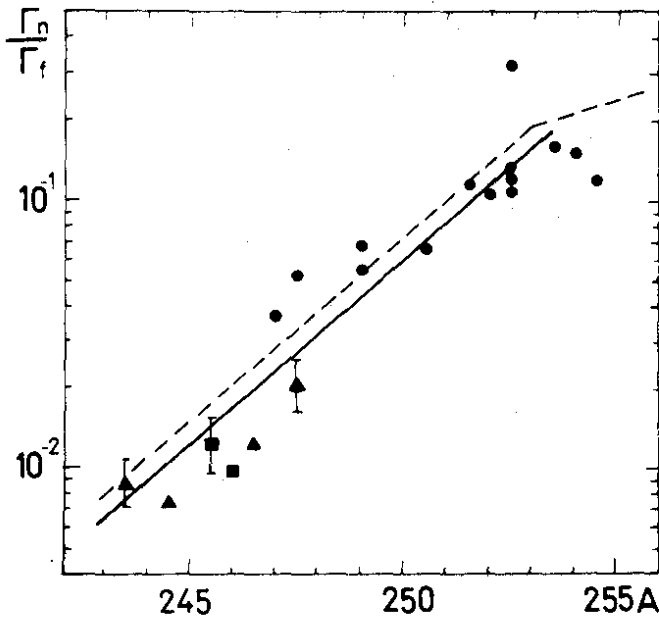


Fig. 6. Nuclear fissility parameter of F_m as a function of mass number A . The circles show the experimental data obtained with C , N , O and Ne ions; the squares are our data, and the triangles are the data from ref.^{1/} for the reaction $Pb(Ar, xn)$. The solid line shows the results of calculation using eq. (11), the dashed line is an empirical relation from ref.^{14/}

REFERENCES

1. Yu.Ts.Oganessian, A.S.Iljinov, A.G.Demin and S.P.Tretyakova. Nucl.Phys., A239 (1975) 353.
2. Yu.Ts.Oganessian, A.G.Demin, A.S.Iljinov, S.P.Tretyakova, A.A.Pleve, Yu.E.Penionzhkevich, M.P.Ivanov, and Yu.P.Tretyakov. Nucl.Phys., A239 (1975) 157.

3. G.M.Ter-Akopian, A.S. Iljinov, Yu.Ts.Oganessian, O.A.Orlova, G.S.Popeko, S.P.Tretyakova, V.I.Chepigin, B.V.Shilov, and G.N.Flerov. Nucl.Phys., A255 (1975) 509.
4. G.N.Flerov, Yu.Ts.Oganessian, A.A.Pleve, N.V.Pronin, Yu.P.Tretyakov. Nucl.Phys., A267 (1976) 559.
5. Yu.Ts.Oganessian, A.G.Demin, N.A.Danilov, G.N.Flerov, M.P.Ivanov, A.S. Iljinov, N.N.Kolesnikov, B.N.Markov, V.M.Plotko, and S.P.Tretyakova. Nucl.Phys., A273 (1976) 505.
6. Yu.Ts.Oganessian, Yu.P.Tretyakov, A.S. Iljinov, A.G.Demin, A.A.Pleve, S.P.Tretyakova, V.M.Plotko, M.P.Ivanov, N.A.Danilov, Yu.S.Korotkin, and G.N.Flerov. Pisma JETP 20 (1974) 580.
7. M.Nurmia, T.Sikkeland, R.Silva, and A.Ghiorso. Phys.Lett., 26F (1967) 78.
8. L.Northcliffe, and R.Schilling. Nucl. Data Tables, 7 (1970) 233.
9. T.Sikkeland, J.Maly, D.F.Lebeck. Phys. Rev., 169 (1968) 1000.
10. A.S. Iljinov, JINR, P7-7108, Dubna, 1973.
11. Yu.Ts.Oganessian, Yu.E.Penonzhkevich, K.A.Gavrilov, and Kim De En. JINR, P7-7863, Dubna, 1974.
12. H.H.Gutbros, W.G.Winn, and M.Blann. Nucl.Phys., A213 (1973) 267.
13. A.S. Iljinov and V.D.Tonejev. Yad.Fiz., 9 (1968) 48.
14. T.Sikkeland, A.Ghiorso, and M.T.Nurmia. Phys.Rev., 172 (1968) 1232.

Received by Publishing Department
on July 21, 1977.